

# Development of a 4096 Element MEMS Continuous Membrane Deformable Mirror for High Contrast Astronomical Imaging

S.A. Cornelissen<sup>1</sup>, P.A. Bierden<sup>1</sup>, T.G. Bifano<sup>1,2</sup>

<sup>1</sup>Boston Micromachines Corporation, 108 Water St, Watertown, MA 02472, (617)926-3948, [SAC@bostonmicromachines.com](mailto:SAC@bostonmicromachines.com), (617)926-8796, [PAB@bostonmicromachines.com](mailto:PAB@bostonmicromachines.com).

<sup>2</sup>Boston University, 15 St. Mary's St., Brookline, MA 02446, (617) 353-5619, [tgb@bu.edu](mailto:tgb@bu.edu)

## ABSTRACT

Presented in this paper is the development of a 4096 element continuous membrane deformable mirror under development for the Gemini Planet Imaging instrument designed for extra solar planet detection. This deformable mirror will enable the next generation of adaptive optics (“Extreme” AO) capable of achieving contrasts of up to  $10^8$ , required to detect these planets that are obscured by the brightness of its parent star. This surface micromachined MEMS deformable mirror will have an active aperture of 25.2mm consisting of thin silicon membrane mirror supported by an array of 64x64 electrostatic actuators exhibiting no hysteresis and sub-nanometer repeatability. This deformable mirror will be capable of 4 $\mu$ m of stroke, have a surface finish of <10nm RMS with a fill factor of 99.8%, and be capable of frame rates in excess of 2.5kHz. This development effort combines new design features, fabrication processes and packaging methods with those developed for commercially available 1024 and 140 element MEMS deformable mirrors to achieve unprecedented performance and reliability.

Keywords:

Deformable mirror, MEMS, adaptive optics

## 1. INTRODUCTION

An extra solar planet imaging instrument, using high-contrast adaptive optics, is under development for the 8 meter Gemini telescope. This instrument, the Gemini Plane Imager (GPI), will use a microelectromechanical (MEMS) based deformable mirror to achieve contrast ratios of  $10^7$ - $10^8$  required to detect Jupiter-like planets outside of our solar system that are a billion times fainter than the sun and obscured by light from its parent star, atmospheric aberrations, and optical imperfections in the imaging systems<sup>1</sup>. MEMS DMs are a desirable choice for many imaging systems due to their inherent small size, high speed, and low cost relative to macro-scale DMs while maintaining comparable optical performance<sup>2</sup>. In an experimental “Extreme Adaptive Optics” testbed a 1024 element MEMS deformable mirror was characterized to determine if the technology is suitable for this application. The testbed showed that the MEMS DM could be flattened to less than 1nm RMS within controllable spatial frequencies over an aperture of 9.2mm with an average long term stability of less than 0.18nm RMS phase<sup>3</sup>, thereby demonstrating that the MEMS DM is a feasible wavefront compensator for high contrast imaging. A 4096 element MEMS DM with a stroke of up to 4 $\mu$ m, and a surface figure of 10nm RMS is required for the GPI instrument. Although MEMS DMs with array sizes up to 32x32, and 4 $\mu$ m stroke, and 10nm RMS surface quality have been demonstrated they have not all been achieved on the same device. The development reported here aims to extend the design, fabrication, and packaging processes used to successfully produce Boston Micromachines Corporation’s kilopixel and long-stroke (12x12) MEMS deformable mirrors.

## 2. MEMS DMs

Boston Micromachines’ MEMS deformable mirrors are based on the surface- micromachined, poly-silicon double cantilever actuator architecture pioneered at Boston University<sup>4</sup>, illustrated in Figure 1. The device structure consists of actuator electrodes underneath a double cantilever flexure, the actuator, which is electrically isolated from the electrodes and maintained at a ground potential. The actuators are arranged in

a square grid, on a pitch of 300-400 $\mu\text{m}$ , and the flexible mirror surface is connected to the center of each actuator through a small attachment post that translated the actuator motion to a mirror surface deformation.

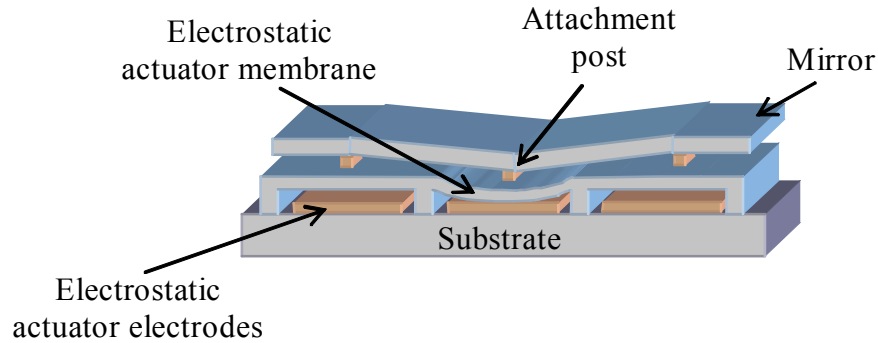


Figure 1. Cross-section of 1x3 electro-statically actuated MEMS deformable mirror.

This MEMS DM architecture allows for local deformation of the mirror membrane since a single actuator only influences its near neighbors and therefore does not cause deformations over the entire aperture as is the case with membrane mirrors. High-order aberrations in the optical path can therefore be corrected using these DMs. Figure 2 shows surface measurements of the DM with a single actuator, as well as with a pattern of actuators deflected.

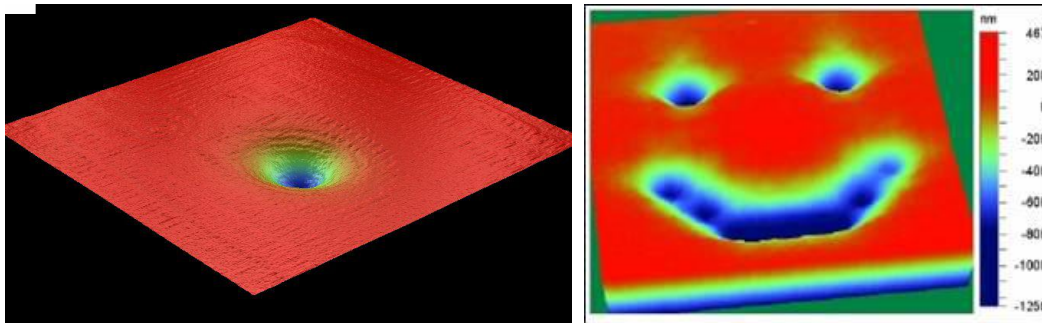


Figure 2. Image of an optical surface measurement of a 144 element DM with a single pixel actuated (left). The influence of the single element deflection only affects its immediate neighbors leaving the rest of the mirror surface unchanged. This local influence characteristic of the DM allows for high-order and otherwise arbitrary shapes on the DM (right).

### 3.1 DM actuation

Electrostatics is used to achieve mirror deformation at each actuation point. The actuator has an initial gap,  $g$ , between the flexure and the fixed electrode. An applied potential,  $V$ , results in an attractive electrostatic force that bends the actuator membrane downward. As the flexure bends, an elastic (mechanical) restoring force acts in the opposite direction. At equilibrium these two forces balance and the equilibrium deflection at the membrane mid-span is  $z$ . The equilibrium deflection is a nonlinear increasing function of  $V$ . Until the voltage is raised to a point where the equilibrium deflection is equal to a little more than one third of the initial gap, the equilibrium is stable. Above that voltage, electrostatic forces are so large that they cannot be balanced by mechanical restoring forces, and the actuator membrane crashes unstably into the fixed electrode. In practice, this unstable region is generally avoided. Fundamentally a parallel plate electrostatically driven actuator can only travel one-third of the gap between the flexure and the electrode before the instability is reached.

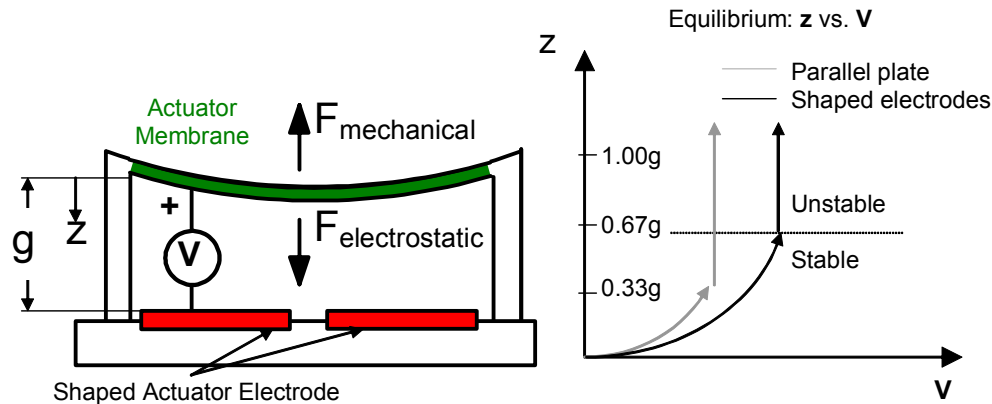


Figure 3. Schematic of electrostatic actuation of a double cantilever flexure used in the MEMS DM design.

To achieve longer stroke using this device architecture a shaped electrode design is used that eliminates the electrostatic attractive force beneath the area of the actuator membrane in which the separation between the flexure and electrode are smallest. Shown schematically in Figure 3, this shaped electrode actuator achieves higher stroke at a cost of a higher actuation voltage for a given actuator geometry. Using small perforations, the mechanical stiffness of the actuator is modified to reduce the maximum operating voltage of the DM to the desirable level.

### 3.2 MEMS DM fabrication process

The MEMS DMs are fabricated using surface micromachining batch-fabrication techniques. The custom fabrication process, illustrated in figure 4, uses three structural layers of poly-silicon (poly) alternating with two sacrificial layers of phosphosilicate glass (PSG). For batch processing, 150mm diameter silicon wafers are used as substrates. A low stress silicon nitride layer is deposited, lithographically patterned, and etched to allow electrical access to the substrate.

The first layer of poly-silicon, *poly0*, is deposited, patterned, and etched to create actuator base electrodes and wire routing for the array. The sacrificial PSG layer, *oxide 1*, is deposited, patterned, and etched. The thickness of this film may vary depending on the desired stroke of the device. Another layer of poly-silicon, *poly1*, is deposited, patterned, and etched to create anchors and compliant actuator membranes.

A second, sacrificial PSG layer, *oxide2*, is deposited and chemopolished to remove undesired topography resulting from features etched in the underlying layers. The chemopolish process greatly improves the surface finish of the final poly-silicon mirror layer. *Oxide 2* is then patterned, and etched to create mirror post attachment points and to serve as a spacer between the actuator and the mirror, providing sufficient clearance for the mirror membrane for its  $6\mu\text{m}$  range of motion. A final poly-silicon layer, *poly2*, is deposited, patterned, and etched to create the mirror and its post attachments to the *poly1* actuator. The *poly2* film touch polished using CMP to further improve the optical quality of the mirror surface. Pad metal is patterned and deposited through a liftoff process to facilitate wire bonding of the device. Sacrificial material is removed with a hydrofluoric acid etch, releasing the structural poly-silicon.

This fundamental device design and fabrication process has been used to produce 144 element deformable mirrors, capable of up to  $4\mu\text{m}$  of stroke, that have been successfully used to improve resolution in a variety of imaging systems for vision science and microscopy systems. The first commercially available MEMS kilopixel ( $32 \times 32$  actuators) deformable mirror was also developed from this technology for laser communication, and terrestrial and space-based astronomical imaging systems. The advances made in the development of these MEMS DMs lay the foundations for the realization of the 4096 element deformable mirror since it will combine the  $4\mu\text{m}$ .

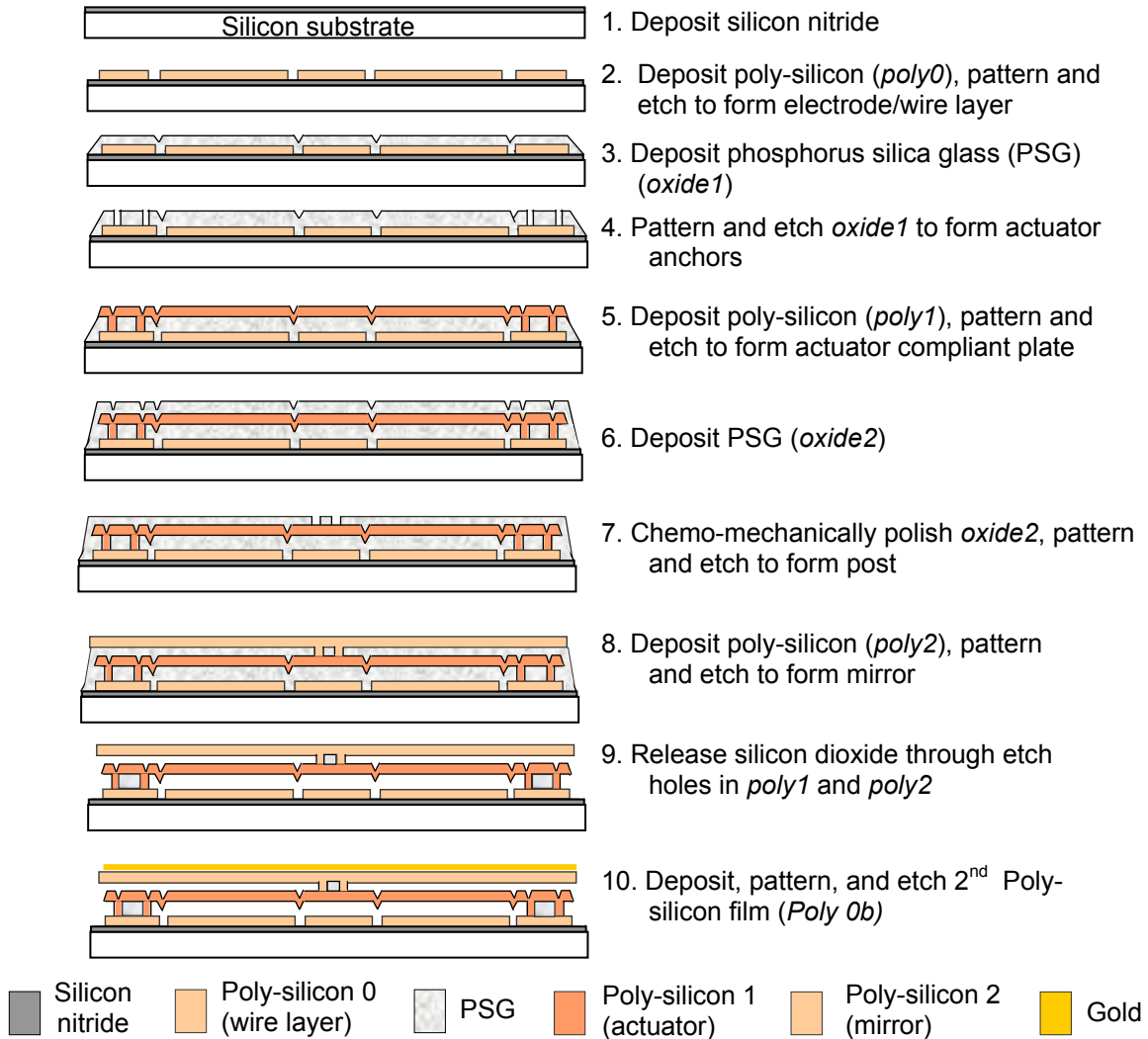


Figure 4. Fabrication process flow used to manufacture Boston Micromachines' MEMS DMs. A cross-section of a single actuator is shown.

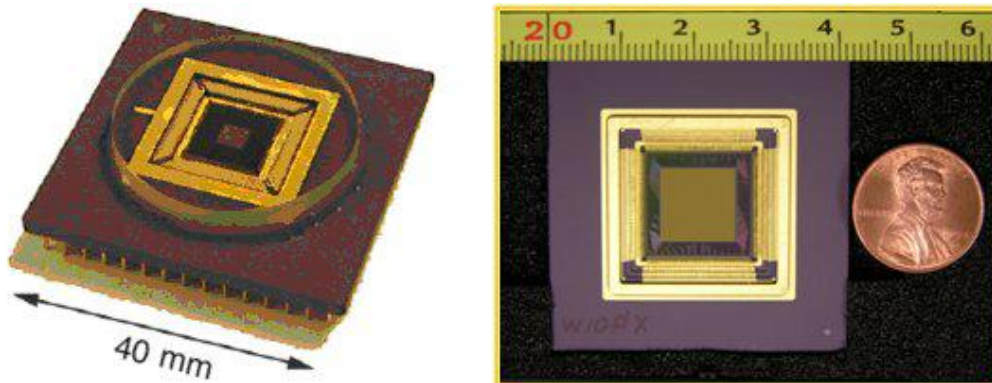


Figure 5. Boston Micromachines 140 (left) and 1024 element (right) deformable mirrors

#### 4. 4096 ELEMENT MEMS DM DESIGN

Table 1 lists the device requirement to enable high-contrast imaging in the Gemini Planet Imager. Although some of these parameter have been achieved on existing Boston Micromachines MEMS DMs, they have not all been achieved simultaneously on a single device.

Table 1. 4096 Element MEMS Deformable Mirror Requirements

Description	Requirement
Pixel count	4096 (64x64 array)
Square Pitch	300 to 400 $\mu\text{m}$
Stroke	2-3 $\mu\text{m}$ , after mirror is fully flattened to within 70 (RMS)
Fill Factor	99%
Active Aperture size	19.2 mm (48 actuator diameter @ 400 $\mu\text{m}$ pitch)
Pixel surface finish (RMS)	<10 nm
Pixel surface finish (P-V)	3 times "Pixel surface finish (RMS)"
Flatness over aperture	<70 nm (tilt & sphere removed) (RMS)
Bandwidth	~2.5 kHz
Inter-Actuator Stroke	1 $\mu\text{m}$
Yield	100% of actuators on a 48 actuator diameter circular aperture function to spec.
Operating Temperature	-30C

#### 4.1 Scaling to a 64x64 array

Although the Boston Micromachines MEMS DM mechanical architecture can be scaled to the 64x64 array size a new wire routing scheme is required to allow 4096 wire traces to reach the individual actuator electrodes while maintaining the required pitch. A buried wire process was developed such that the actuator electrodes and wiring are on two separate poly-silicon layers, with the electrically conductive Poly0a wires between two Silicon Nitride Dielectric layers. This increases the effective area that may be used for wire routing and also allows for the wires to have more width, increasing device yield by making these critical features less sensitive to defects during the fabrication process. This wiring scheme is illustrated in figure 6. Following the fabrication of the electrical layers the manufacturing process will follow the same steps illustrated in figure 4.

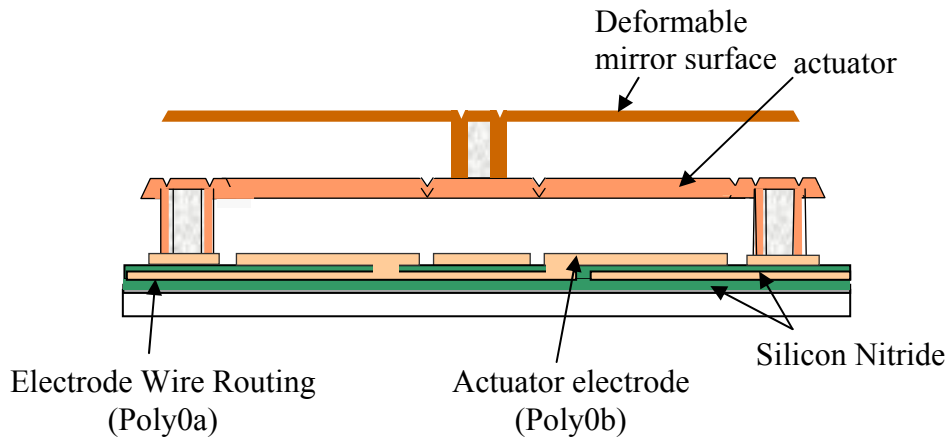


Figure 6. Cross-section of a single deformable mirror pixel using a buried poly-silicon wiring layer to address the actuator electrode.

Since the electrode wire traces are routed underneath the actuator array, ground planes were added to the Poly0b layer to eliminate potential cross talk between actuators due to charging of the silicon nitride films. In prototype fabrication runs, this routing scheme was demonstrated to function properly with no measurable cross talk between actuators. An interferometric image of this prototype device is shown in Figure 7, in which one actuator is pulled down using 120V. No deflection is measurable on any non-addressed actuators.

## 4.2 Baseline device performance

The stroke, bandwidth, and surface finish requirements for the 4096 element deformable mirror pose challenges for the actuator design since each of these performance parameters affect the others. Increasing stroke requires a decrease in actuator stiffness for a given voltage, which therefore reduces the overall bandwidth of the DM. Reducing the stiffness of the actuator also affects the optical quality of the device since the small perforations in the actuator “print-through” onto the mirror. Print-through effects are caused by the conformal nature in which the thin poly-silicon and PSG films are deposited.

To achieve the desired stroke of 2-3 $\mu\text{m}$  after the mirror is fully flattened, a 4 $\mu\text{m}$  stroke actuator design on a 400 $\mu\text{m}$  pitch, was chosen. This will provide sufficient stroke in the DM to meet this goal and allow the device to operate with sufficient margin over its critical deflection. As shown in Figure 8, over 4 $\mu\text{m}$  of stroke has been achieved with Boston Micromachines DMs that were developed for retinal imaging applications.

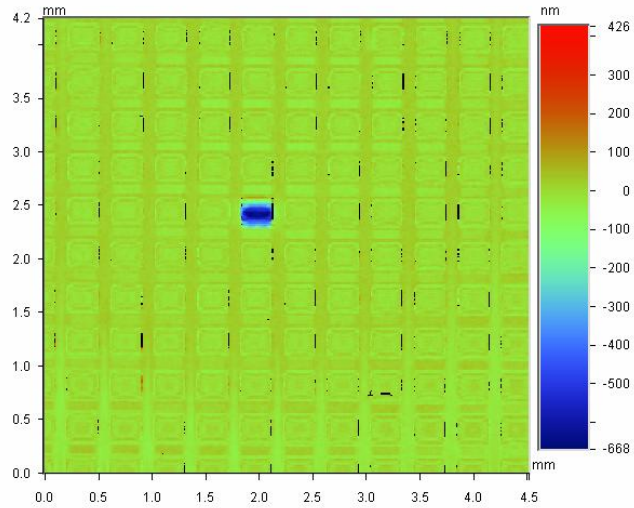


Figure 7. Interferometric image of 11x10 sub-array of actuators on a prototype 64x64 device. A single pixel is addressed in the center of the array (120V) without cross-talk between actuators

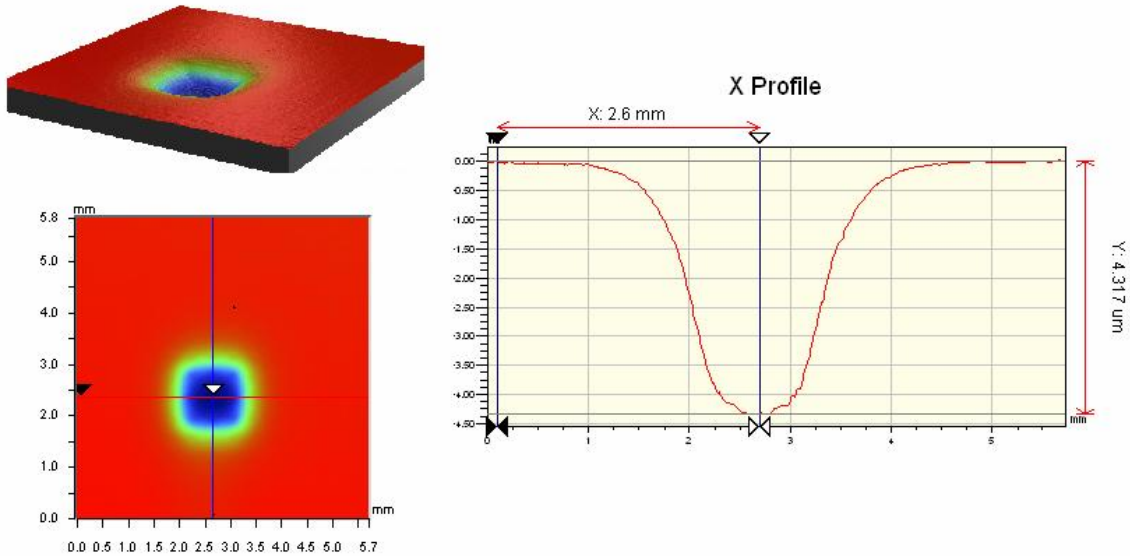


Figure 8. Measurement of 144 element MEMS DM in which a 3x3 array is pulled down to over 4 $\mu\text{m}$  of deflection

The inter-actuator stroke of this 4 $\mu\text{m}$  stroke device meets the 1 $\mu\text{m}$  requirement. To demonstrate this, a large area of the 12x12 device was pulled down to approximately half of its maximum deflection. The deflection of two neighboring pixels in the area were then modified such that one moved to its maximum deflection and the other to its minimum deflection (i.e. max voltage and 0 voltage applied respectively). The results of this measurement are shown in Figure 9.

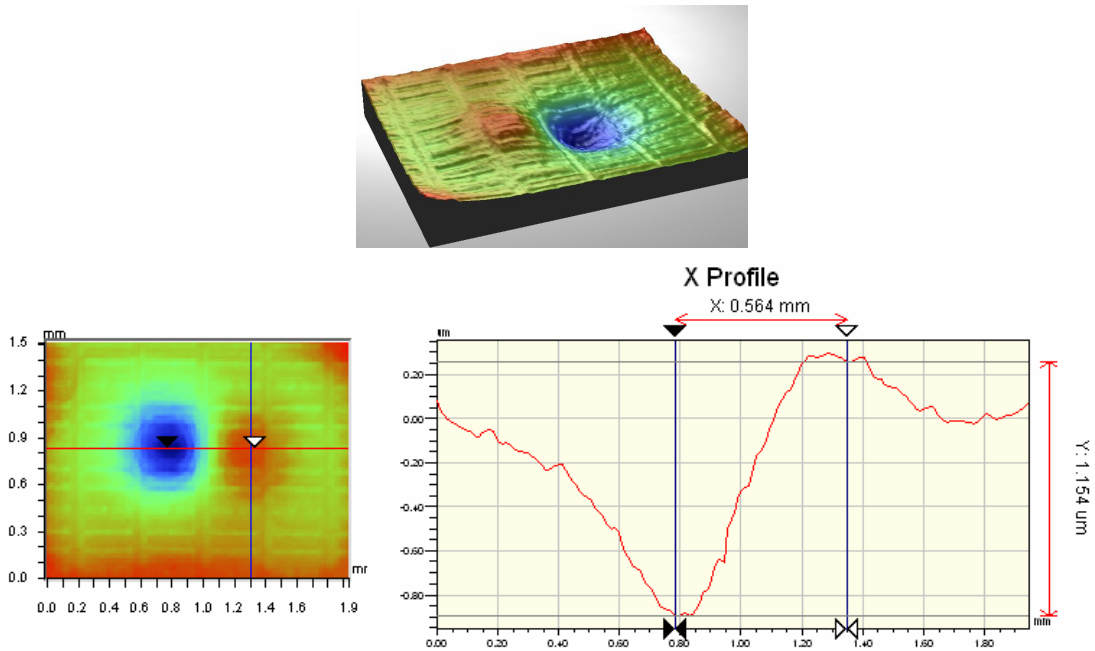


Figure 9. The inter-actuator stroke between two neighboring elements on the baseline MEMS deformable mirror design was measured to be  $1.15\mu\text{m}$ .

These devices have also been measured to have a response time that meets the requirements for the 64x64 device. Using a Laser Doppler Vibrometer the frequency response was measured. The control bandwidth for the device was measured to be  $\sim 2.8\text{kHz}$  (see figure 10).

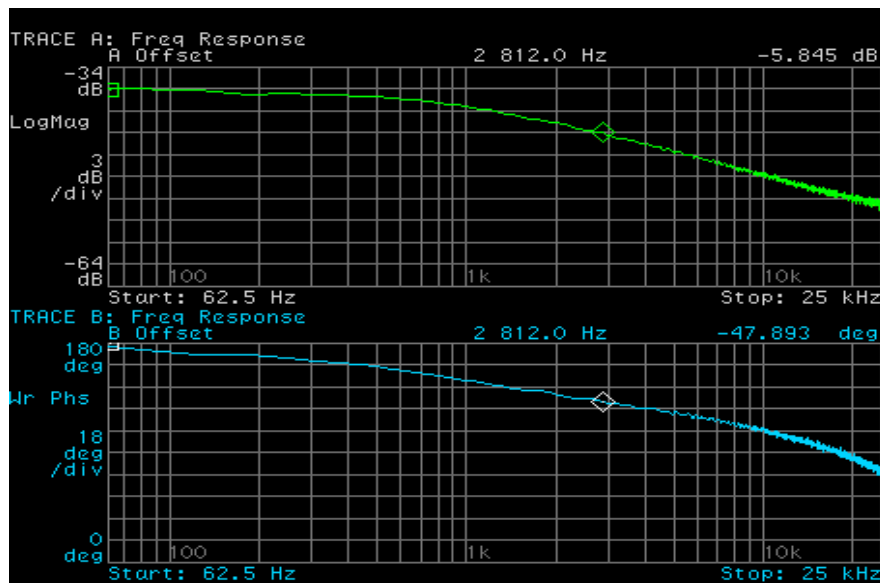


Figure 10. Dynamic response of 140 element,  $4\mu\text{m}$  stroke DM. The control bandwidth, indicated by the 6dB down point, is measured to be  $\sim 2.8\text{kHz}$  (calculated as  $20\log(v_2/v_1)$  where  $v_2$  is the LDV displacement output voltage, and  $v_1$  is the HP source voltage, therefore  $-6\text{dB}$  corresponds to  $v_2/v_1=0.5$ ). The phase lag is  $\sim 48^\circ$  at this frequency.

The surface finish of this device, shown in figure 11, is approximately twice the required value. The effect of the perforations in the actuator, used to achieve the long stroke, is clearly visible on the mirror surface. This compares to a shorter stroke,  $300\mu\text{m}$  pitch device that does not use this actuator design, with which a pixel surface of less than  $9\text{nm}$  RMS can be achieved.

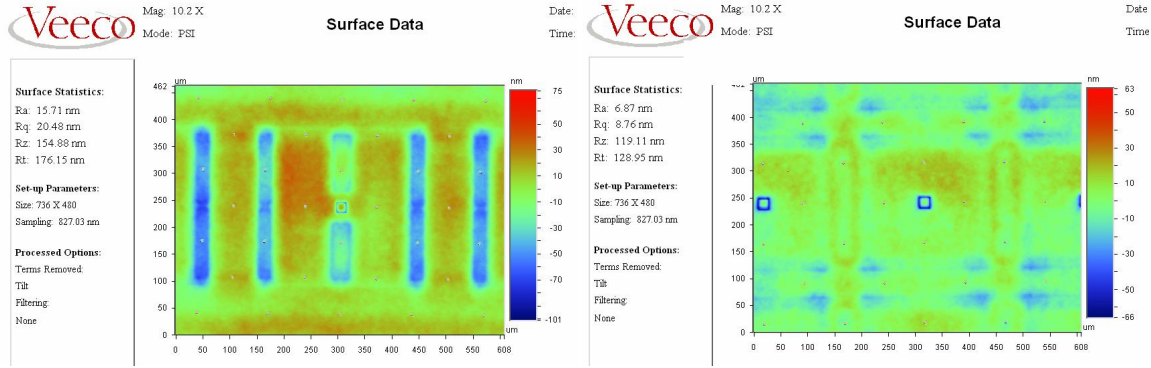


Figure 11. Pixel surface roughness measurements of 400µm pitch, 4µm stroke DM (left) and 300µm pitch, 2µm stroke DM (right). A surface finish of ~20nm RMS and 9nm RMS is achieved on the DM using these actuator designs respectively.

The surface measurement of these devices also show the high fill factor of the Boston Micromachines DMs, which is greater than 99.8%. The fill factor is limited by a small number of etch access holes in facesheet of the mirror required for the fabrication of the devices are located on.

### 4.3 Device performance predictions

To improve the surface quality, modifications to the actuator design were considered that would not only minimize print-thru effects but would also provide the required stroke. Using finite element analysis, new actuators were designed that balanced the actuator perforation size, flexure span, electrode shape, operating voltage, and natural frequency.

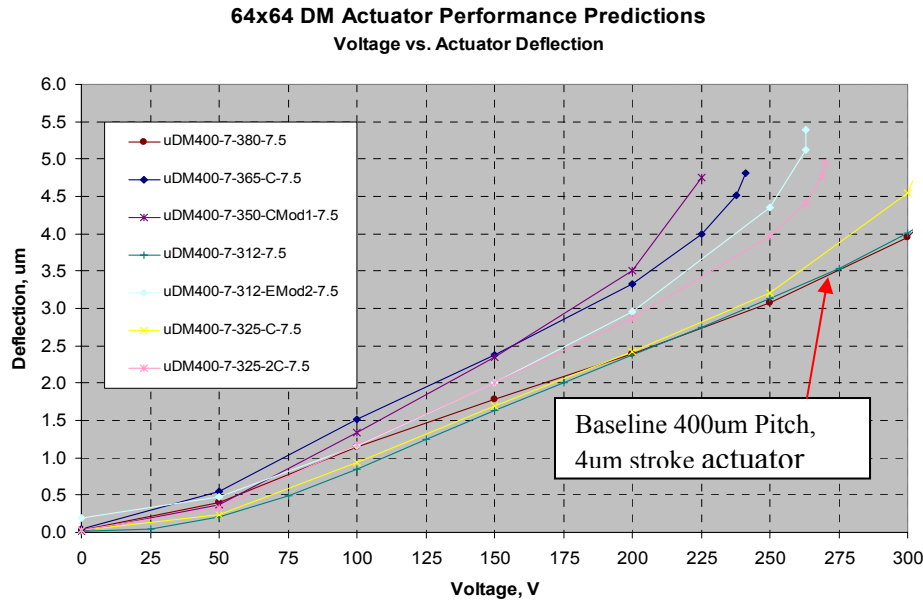


Figure 12. Voltage vs. Deflection performance predictions for 4096 element MEMS DM.

The analysis showed that improved performance could be achieved by modifying these parameters compared to the baseline 4µm stroke device. The predicted voltage vs. deflection performance of these devices is shown in Figure 12. The natural frequency of these actuators, listed in Table 2, was compared to the baseline design as a measure of DM bandwidth. Two out of the six modified actuator had a lower natural frequency than the baseline device; the other were up to 43% higher.

Table 2. Comparison of Actuator natural frequencies

Actuator Design	1 <sup>st</sup> Mode (KHz)	% Increase from heritage design
μDM400-7-312 (Heritage)	54	-
μDM400-7-380	59	9%
μDM400-7-365-C	50	-7%
μDM400-7-350-2C	53	-2%
μDM400-7-350-C	59	9%
μDM400-7-325-2C	68	26%
μDM400-7-325-C	77	43%

#### 4.5 Initial results

A sample of devices from a fabrication run, designed to determine the final manufacturing processes and device design that will be used for the 4096 element DM, have been evaluated for surface figure and actuator stroke. The pixel surface figure of the DM for two of the new actuator designs is shown in figure 13. This surface measurement shows that a surface finish of less than 10nm RMS has been achieved using the modified actuator design. Although the underlying actuator cuts are still visible on the surface, the magnitude of the print-through has been reduced by changing the size of these perforations such that dishing effects caused by chemomechanical polishing steps has been reduced.

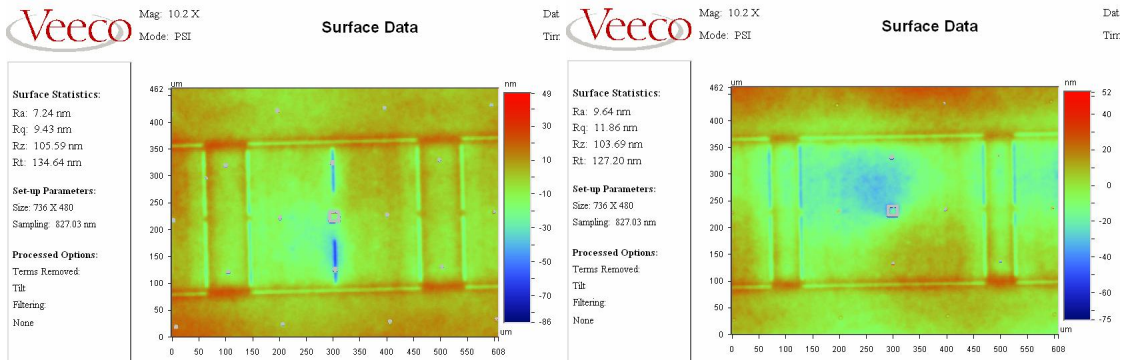


Figure 13. Surface figure measurements of two DMs with modified actuator design; Left – actuator 325-2C; Right – actuator 350-C. The actuator perforation modifications have reduced the surface figure to below 10nmRMS.

The electromechanical performance of the actuators was tested by applying a known voltage to a single actuator and measuring the displacement using a WYKO interferometer. The results are shown in Figure 14. Most of these devices achieved a stroke of 4μm at a voltage below 250 volt. The total stroke was lower than predicted due to an initial downward bow in the actuator (up to 1.6μm on some devices) due to a high compressive stress in the poly-silicon actuator film induced by excessive bow in the substrate. This effect may be reduced by removing some of the thin films off the back of the wafer to more closely match the film stresses each side of the wafer.

A 4096 device with limited functionality was also fabricated to investigate the effects of the large DM on the fabrication process. Actuators were coupled together in groups of various sizes to get an indication of actuator yield on a single device. It was found that out of 1500 actuators test, 100% were responsive with 2 actuators having small lithography defects that limited the total stroke. A Zygo interferometer was used to characterize the surface of the device, shown in figure 15. This DM has two non-active rows around the 64x64 array to reduce edge effects and to allow reliable operation of all 4096 actuators. A low-order spherical surface figure is present on the surface with a peak to valley of ~600nm. This is caused by CMP steps in the fabrication process. Although this may be corrected for by a low-order “woofer” DM in the GPI instrument corrective actions for these surface effects are being investigated.

**64x64 DM Actuator Performance Measurements**  
Voltage vs. Actuator Deflection

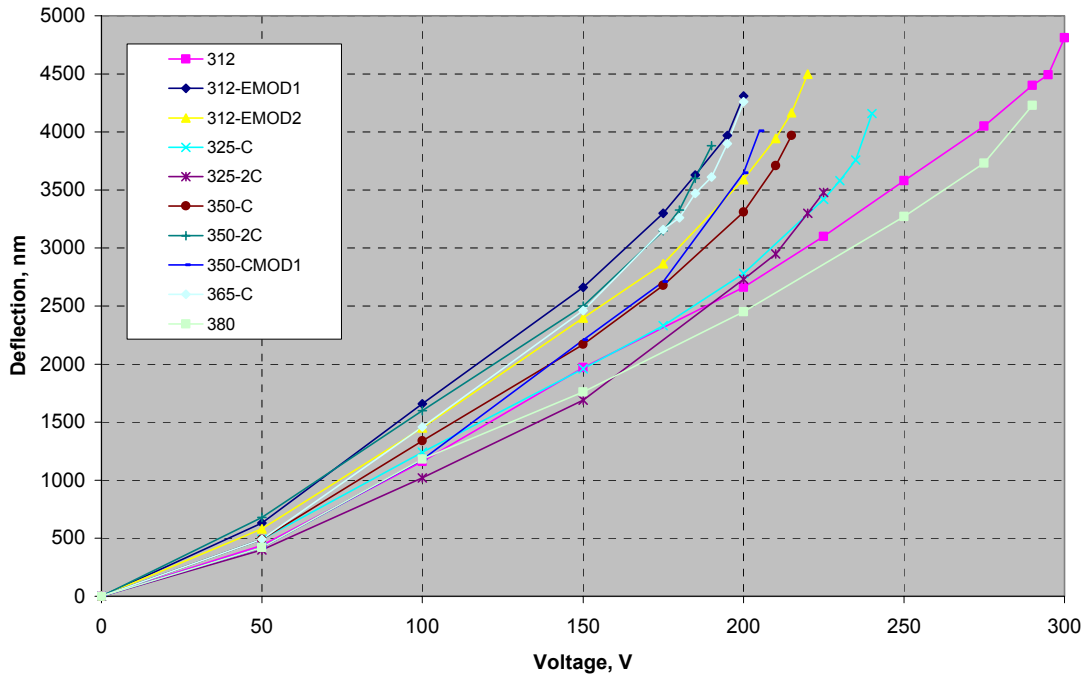


Figure 14. Voltage vs. deflection characteristics measured from first set of actuators from the first device development fabrication run

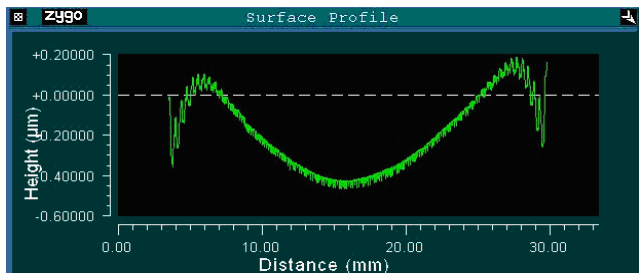
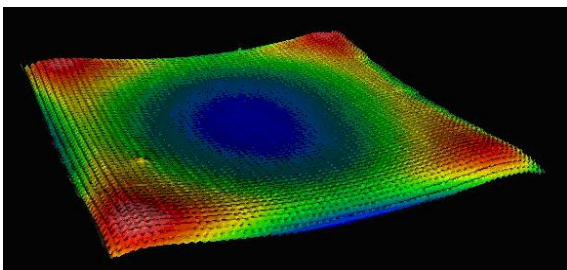
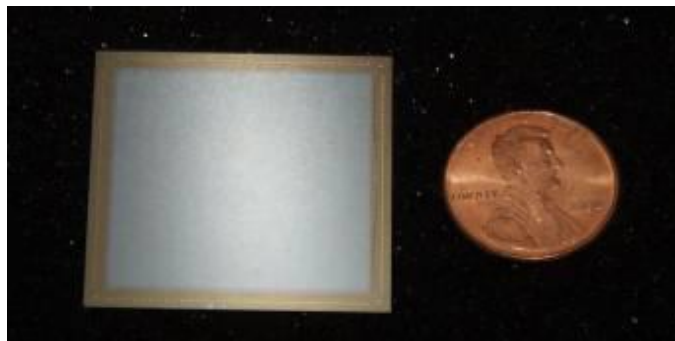


Figure 15. A Prototype of 4096 element MEMS deformable mirror -68x68 array with central 64x64 array active (top). A measurement of the overall surface figure of this device shows a P-V surface variation of ~600nm (bottom).

## 5. PACKAGING

The device will be mounted in a custom ceramic Land Grid Array (LGA) package that provides the 4096 interconnects to the drive electronics. The DM will be wirebonded in this package, using bondpads located on the periphery of the 48mm die, to provide electrical signals to the DM. To allow for operation of the device at an operating temperature of -30C, the silicon substrate of the DM will require a new mounting technique to minimize the effects of CTE mismatch between the die and the ceramic chip carrier. Since the die has a fairly large size, the mounting process must be performed carefully such that the surface figure of the DM is not affected. Preliminary test performed on an unmounted prototype 64x64 DM, and smaller 12x12 DMs shows that the surface figure and electromechanical performance is not significantly affected at these low temperatures indicating that the main engineering challenge for operating at low temperatures is how to mount this large DM to its carrier.

## 6. CONCLUSION

The best performance characteristics and fabrication processes used for Boston Micromachines' commercial MEMS deformable mirrors are being combined to produce the first 4096 element MEMS deformable mirror that will enable high contrast imaging instruments seeking to image extra solar Jovian planets. Modifications made to existing actuator designs have proven effective to improve surface quality while maintaining 4 $\mu$ m of actuator stroke, and reducing the overall operating voltage. Further development work is ongoing to improve stress characteristics to optimize the actuator performance and DM surface figure.

## REFERENCES

1. Macintosh, B., Graham, J., Oppenheimer, B., Poyneer, L., Sivaramakrishnan, A., Veran, J., "MEMS-Based Extreme Adaptive Optics for Planet Detection", Proc. SPIE Vol. 6113, 611308 (Jan. 23, 2006)
2. Doble, N., Yoon, G., Chen, Li, Bierden, P. A, Olivier, S., and Williams, D., "Use of a microelectromechanical mirror for adaptive optics in the human eye," Optics Letters, 27 (17), pp. 1537-1539, 2002
3. Evans, J., Morzinski, K., Severson, S., Poyneer, L. Macintosh, B., Dillon, D., Reza, L., Gavel, D., Palmer, D., Olivier, S., and Bierden, P, "Extreme adaptive optics testbed: performance and characterization of a 1024-MEMS deformable mirror", Proc. SPIE Vol. 6113, 61130I (Jan. 23, 2006)
4. Bifano, T., Perreault, J., Mali, R., et al., "Microelectromechanical deformable mirrors", IEEE J. of Selected Topics in Quantum Electronics, 5 (1): 83-89 Jan-Feb 1999.